Modelling vegetation water-use and groundwater recharge as affected by climate variability in an arid-zone *Acacia* savanna woodland

Chao Chen[1,2*] Derek Eamus[1,2,3,4] James Cleverly[2,4] Nicolas Boulain[2] Peter Cook[1,5]

[1]National Centre for Groundwater Research and Training (NCGRT), School of Environment, Flinders University, Adelaide, SA, 5001, Australia

[2]Plant Biology and Climate Change Cluster, University of Technology Sydney, PO Box 123, Broadway, NSW 2007, Australia

[3]NCGRT, University of Technology Sydney

[4]Australian Supersite Network, Terrestrial Ecosystem Research Network, University of Technology Sydney

[5]Water for a Healthy Country National Flagship, Commonwealth Scientific and Industrial Research Organisation, Division of Land and Water, Glen Osmond, Adelaide, SA 5064, Australia

[*] Corresponding author (chao.chen@uts.edu.au)

Abstract

(1) For efficient and sustainable utilization of limited groundwater resources, improved understanding of how vegetation water-use responds to climate variation and the corresponding controls on recharge is essential. This study investigated these responses using a modelling approach. The biophysically based model WAVES was calibrated and validated with more than two years of field experimental data conducted in Mulga (*Acacia aneura*) in arid central Australia. The validated model was then applied to simulate vegetation growth (as changes in overstory and understory leaf area index; LAI), vegetation water-use and groundwater recharge using observed climate data for the period 1981−2012. Due to large inter-annual climatic variability, especially precipitation, simulated annual mean LAI ranged from 0.12 to 0.35 for the overstory canopy and 0.07 to 0.21 for the understory. These variations in simulated LAI resulted in vegetation water-use varying greatly from year-to-year, from 64 to 601 mm pa. Simulated vegetation water-use also showed distinct seasonal patterns. Both climate variability and vegetation dynamics exerted significant controls on annual recharge. The simulated annual recharge ranged from 58 to 672 mm when only climate effects were considered; but this range was greatly reduced to 0 to 48 mm when vegetation water-use was accounted for. Understanding such effects under the observed historical climate conditions gave significant insight into assessing potential impacts of interactions amongst climate variability and land use/land cover change on groundwater resources management in arid and semi-arid regions.

1. Introduction

(2) Groundwater is a valuable natural resource, which not only supports human activities, but also has a key role in sustaining the health of wide-spread groundwater dependent ecosystems (*Eamus et al.*, 2006; *Jha et al.*, 2007). Sustainable water resource management is a major challenge for water resource managers in arid and semi-arid regions (*Fernandez et al.*, 2002), where excessive and unsympathetic groundwater abstraction can degrade vegetation health (*Clifton and Evans*, 2001, *Donohue et al.*, 2007). Vegetation dynamics in arid and semi-arid regions largely depend on soil water availability, which in turn, result in a number of complex hydrologic processes (*Gee et al., 1994; Porporato et al., 2002; Scanlon et al., 2005; Garcia et al., 2011*). Climate variations, which lead to changes in vegetation structure and/or its water-use, can have a follow-on impact on recharge to groundwater under vegetation. With increasing demand for water and a changing climate regime, it is crucial to better understand the hydrological role of vegetation for developing sustainable groundwater management and mitigating the environmental impacts of groundwater development. A key aspect of this role is that of transpiration, a major component of catchment water balances, to which biological productivity is intimately coupled (*Berry et al.*, 2005; *Chen et al.*, 2010). Understanding the effects of climate variations on vegetation water-use and groundwater recharge is particularly important in arid and semi-arid Australia, where limited water resource availability already constrains regional development. As climate change is a growing concern in water management globally, including Australia, knowledge of the responses of catchment water balance to local climate is important for developing adaptive climate change strategies and sustainable groundwater resource management.

(3) Studies of these complex problems can be conducted in field conditions and much has been learnt about the relationship between growth, photosynthesis and the water cycle (*Farrington*, 1989; *Thorburn et al.*, 1993; *Zhang and Schilling*, 2006). However, field experiments are time consuming, relatively expensive and difficulties in up-scaling from limited numbers of observations are readily apparent (*Singh et al.*, 2006). To overcome this, process-based models that link hydrology and plant ecophysiology have been developed that provide useful tools to investigate interactions amongst

energy, water and momentum balances of the soil-vegetation-atmosphere system across multiple spatial and temporal scales (*Baird et al.*, 2005; *Guswa et al.*, 2002; *Laio et al.*, 2001; *Zhang et al.*, 1996). Studies of modelling these coupled behaviours have been attempted previously (*Gerten et al.*, 2004; *Kucharik et al.*, 2000). In one such study of the effects of climate on recharge across Australia, numerical modelling showed that the role of climate drivers varies across soil and vegetation types (*Barron et al.*, 2012). *Crosbie et al.* (2011) simulated the effects of climate change on recharge in the Murray-Darling Basin and found that recharge was increased despite a modelled decrease in rainfall and increased temperature. This was a result of reduced transpiration due to the effect of high temperature stress on vegetation growth. In contrast, recharge increased with rainfall when coupled to a 3°C temperature increase in the Upper Nile Basin, but increases in evapotranspiration (ET) lead to reductions in recharge at higher temperature (*Kingston and Taylor*, 2010). Although these studies provide useful information for developing applicable water management practices, there is still a lack of systematic analysis of the effects of climate variability on vegetation water-use and consequential recharge in arid and semi-arid regions.

(4) Mulga (*Acacia aneura* and related species) is a low-to-medium height (2–8 m) tree, dominating arid and semi-arid zones between approximately 20 ^{o}S and 31 ^{o}S in coastal Western Australia and throughout the continental interior. Mulga occupies almost 20% of the Australian continent and overlies many significant aquifers including the Great Artesian Basin. Covering such a large portion of continental Australia, vegetation water-use and recharge beneath the Mulga-dominated woodland are assumed to contribute significantly to regional water budgets (*Eamus et al.*, 2013). Mulga is functionally a savanna as it consists of a discontinuous tree layer over a grassy understory with highly seasonal rainfall. This pattern is more pronounced in arid central Australia where rainfall variability is skewed towards very large event cycles (*Berry et al.*, 2011; *Morton et al.*, 2011) and groundwater is an important water source as a result of unreliable surface water. As such knowledge of the magnitude of recharge is critical to the development of sustainable strategies to allocate limited groundwater. To-date, no studies have investigated the responses of groundwater recharge to climate and Mulga-dominated vegetation in arid and semi-arid regions.

(5) The objective of this study was to produce a detailed mechanistic understanding of the dynamic links between vegetation water-use and climate, and their influence on groundwater recharge through application of a physiologically-based model of the soil-plant-atmosphere continuum. The primary purpose of this study was to test the hypothesis that recharge of groundwater is largely dependent on the rate of water-use of vegetation growing in an arid region of Australia. The aims of this study were to: 1) parameterise the WAVES model to allow simulation of plant growth and water balance components in the Ti-Tree Basin using field data; 2) quantify the responses of plant growth and vegetation water-use to climate variability and the corresponding effects on groundwater recharge.

2. Materials and methods

2.1. Study site and data for model test

(6) This study was performed in the Ti Tree Basin, located 150 km north of Alice Springs, in the Northern Terrority of Australia, and 180 km north of the Tropic of Capricorn (Figure 1). The area of the basin is approximately 5,500 km^2, and comprises undulating sand plains with alluvial deposits along ephemeral drainage lines. Vegetation includes large areas of spinifex under sparse woodland of Bloodwood (Corymbia opaca) and low trees, including *Acacia coriaceae* and *Hakea macrocarpa*. The sand plains contain patches of Mulga scrubland (*Acacia aneura s.lat*.) and the major rivers are lined with River Red Gums (*Eucalyptus camaldulensis var. obtusa*). Due to low rainfall, groundwater in the basin is an important resource for stock, irrigation of small-scale horticultural cropping, and town and community supplies. Over most of the basin, the water table is between 20 and 50 m below the land surface. Recharge to the groundwater needs to be determined to ensure that the resource is properly managed.

(7) The study site is located on the western margin of the Ti-Tree Basin (22.28S, 133.25E, a.s.l. 600 m) (Figure 1). The site is located within a tropical arid zone with hot summers and warm winters. The average rainfall at the nearest meteorological station (Territory Grape Farm Station 015643; 1981–2012 average) is approximately 333 mm, and annual pan evaporation is about 3109 mm. The ecosystem is an *Acacia aneura* (Mulga) savanna woodland with an average canopy height of 6.5 m,

which consists of a discontinuous tree layer over a grassy understory. The soil is characterised as a red kandosol (sand:silt:clay 74:11: 15).

(8) An eddy covariance (EC) tower was located on a flat plain between the Hanson and Woodforde Rivers. This tower is a member of the OzFlux network, which distributes data and maintains data quality standards (*Cleverly, 2011*). Potential fetch is 11 km to the east and 16 km to the south. EC data collection from a 13.7 m tower was initiated on 2 September 2010. Total solar radiation was measured 12.2 m above the ground with a CNR1 (Kipp & Zonen, Delft, The Netherlands). Air temperature and relative humidity were measured 11.6 m above the ground using an HMP45C (Vaisala, Helsinki, Finland). Precipitation was measured with a CS7000 (Hydrologic services, Warwick, NSW, Australia), centred in a 10 m × 15 m clearing at the top of a 2.5 m mast. Frequency of micrometerological measurements was 10 Hz with a 30-minute covariance interval.

(9) Soil samples were collected using a slide hammer (AMS Soil Core Sampler, Envco: The Environmental Collective, Auckland, New Zealand) to extract intact cores (38 mm diameter × 10 cm depth to a maximum depth of 1.4 m) for laboratory analysis. The experimental site has a fairly uniform soil profile and dry bulk density varies only slightly, ranging from 1.67 g cm^{-3} at the surface to 1.86 g cm^{-3} at a depth of 1.4 m. Consequently we assumed that the soil could be simulated as a single layer. Soil hydraulic characteristics required by the model (see below and Table 1) were derived from the ASRIS v1 database (*Johnston et al.*, 2003). Rooting depth of Mulga is generally shallow (likely <5 m depth) and studies indicate that Mulga does not access soil water below 5m, even in drought conditions (*Anderson et al.*, 2008; *Hill and Hill*, 2003). Therefore a soil column of 4 m was chosen considering a relatively shallow rooting depth for Mulga at this site. Soil moisture was measured in two vertical arrays under mulga and understory habitats using TDR probes inserted at the 45^{o} angle (CS610, Campbell Scientific, Townsville, Australia). Insertions were at 10 cm, 60 cm and 100 cm representing average soil moisture across depths of 10–30, 60–80 and 100–120 cm, respectively. All soil measurements were collected on a separate CR1000 and stored on the CR3000 via Pak-Bus communications. Soil moisture measurements were made at the mid-point of each 30-

minute output interval. For model calibration (see below), soil water was averaged without weighting across the two habitat types (Mulga trees and understory grasses).

(10) Leaf area index (LAI) was derived from images acquired with a digital camera (Canon DSLR) equipped with a short focal lens (18 mm). Five 100 m long transects in E, SE, S, SW and W directions were established around the flux tower. Upward and downward images were taken every 10 metres. To compute LAI for the Mulga and the understory, images were acquired with (a) the camera looking to the sky at the nadir (0^o) and (b) inclined down (looking at the soil) at 57.5^o from the vertical (*Weiss et al.*, 2004) for canopy and understory, respectively. These images for canopy were analyzed with a Matlab (Matlab R2012, The Mathworks, Natick, MA, USA) program based on algorithms obtained from *MacFarlane et al.* (2007), and those for understory were analyzed with the CANEYE (version 6.3) software (https://www4.paca.inra.fr/can-eye). Canopy LAI was calculated from the fraction of cover porosity based on the fraction of foliage cover and the fraction of crown cover for each image, while understory LAI was computed and corrected using the clumping index derived from fisheye images, based on the method proposed by *MacFarlane et al.* (2007). Total LAI calculated as the sum of the canopy and understory components was compared to the product MOD15A2 centered on the coordinate of the tower (8-Day Composite (Collection 5), 1 km wide × 1 km length) from the MODIS Land Product Subsets project (http://daac.ornl.gov/MODIS/). To ensure the highest quality, the 8-day composite LAI (Collection5) product was used only when QC filter conditions (FparLai QC < 32) were met.

(11) A more detailed description of the study site and measurements can be found in *Cleverly et al.* (2013b) and *Eamus et al.* (2013).

2.2. Forcing energy-balance closure

(12) Studies of the surface energy balance showed that surface energy fluxes (λE+H; λE: latent heat; H: sensible heat) were frequently underestimated by about 10–30% relative to the surface available energy (Rn-G-S; Rn: net radiation; G: soil heat flux; S: canopy heat storage) (*Constantin et al.*, 1998; *Barr et al.*, 2000, 2001; *Wilson et al.*, 2002; *Li et al.*, 2005). A close examination of flux data

measured in the current study revealed that 24 h average closure rate (D) [D=(H+λE)/(Rn-G-S)] was 74% without accounting for canopy heat storage, which was expected to be relatively minor in short canopies with minimal biomass (*Wilson et al.*, 2002). *Wilson et al.* (2002) accepted flux data for analysis when canopy heat storage was missing, provided that the vegetation height was less than 8m, as observed at our Mulga site. The use of flux data to validate biophysically-based models requires that conservation of energy is satisfied (*Twine et al.*, 2000). Therefore, the measured energy budget must be closed by some method. Here the energy balance was closed each half-hourly period by attributing the residual energy to both H and λE according to the observed Bowen-ratio for that half hourly period.

2.3. WAVES model

(13) WAVES (Water Atmosphere Vegetation Energy and Solutes) is a coupled water and carbon ecohydrological model that predicts dynamic interactions within the soil-vegetation-atmosphere system at a daily time step (*Dawes and Hatton*, 1993; *Zhang et al.*, 1996). In WAVES, soil water movement in both the unsaturated and saturated zones is simulated using a fully finite difference numerical solution of the Richards equation (*Berry et al.*, 2005). Modelling of the unsaturated zone using the Richards equation allows water movement in the soil profile to be modelled under dry conditions. For each soil type, an analytical soil model proposed by *Broadbridge and White* (1988) was employed to describe the relationships among water potential, volumetric water content and hydraulic conductivity. Evapotranspiration was estimated by the Penman-Monteith approach (*Monteith and Unsworth*, 2008). Leaf stomatal conductance was calculated by the equation developed by Ball and Leuning (*Ball*, 1987; *Leuning*, 1995), which was scaled to canopy scales using the method proposed by Sellers (*Sellers et al.*, 1992). The micrometeorological feedback of the sensitivity of transpiration to a marginal change in stomatal conductance at the stand level is regulated by a dimensionless decoupling coefficient proposed by *McNaughton and Jarvis* (1991). The rate of plant growth in the presence of different availabilities of light, water and nutrients was estimated by an integrated rated methodology of *Wu* (1994), which is an empirical model without resolving the details

of chemical and mechanical controls on photosynthesis. Water is extracted for transpiration by roots, which is distributed along the root profile according to root density distribution and water availability in each soil node (*Ritchie et al.*, 1986). The WAVES model is able to simulate plant physiology, which allows changes in environmental factors (temperature, solar radiation, rainfall) to impact water use by vegetation and recharge. WAVES predicts the dynamic interactions and feedbacks between these processes. Thus, the model is well suited to investigations of hydrological and ecological responses to changes in land management and climatic variation. WAVES emphasises the physical aspects of soil water fluxes physiological control of water loss through transpiration. It can be used to simulate the hydrological and ecological effects of scenario vegetation management options (e.g. for recharge control), or the water balance implications of changed climatic conditions. A more detailed modelling strategy and description of WAVES is provided in *Dawes et al.* (1998), *Zhang and Dawes* (1998) and *Zhang et al.* (1996). Most recently, WAVES has successfully reproduced field observations at a point scale (*Dawes et al.*, 2002; *Crosbie et al.*, 2008; *Martin et al.*, 2008; *Cleverly et al.*, 2013b) and has been used to investigate trends in recharge under different soil and vegetation combinations at regional scales (*Crosbie et al.*, 2010, 2011, *Barron et al.*, 2012).

(14) WAVES requires three types of data for parameterisation: meteorology, soil and vegetation. The meteorological data required include daily maximum and minimum temperatures, average vapour pressure deficit, precipitation, precipitation duration, and total solar radiation. The soil data include information on soil layering, along with several hydraulic parameters: soil water conductivity K_s (m d^{-1}), saturated water content θ_s (m^{-3} m^{-3}), air-dry volumetric water content θ_d (m^{-3} m^{-3}), length of capillary λ_c (m), and characteristic soil water retention curve *C*. The Broadbridge-White soil model was used to generate a file containing a table of values of soil-water potential, water content, and hydraulic conductivity to allow WAVES to simulate the movement of soil water with the Darcy-Richard's equation.

226 **2.4. Model calibration and application**

227 (15) Before model calibration, prior vegetation parameters for the Mulga site were adapted from the
228 recommended values for eucalypt trees and for summer annual pastures for the understory habitats
229 contained in the WAVES manual (*Dawes et al.*, 1998). The WAVES model was further calibrated
230 with MODIS and observed LAI, field-measured soil water content and ET during September 2010–
231 August 2011. The vegetation parameters were subsequently modified following calibration and their
232 derived values for the Mulga and understory habitats are listed in Table 2. The calibrated model was
233 then validated using the experimental eddy covariance flux data during September 2010–December
234 2012.

235 (16) Three statistical parameters were used to quantify model performance. These were: 1) the
236 coefficient of determination for $y = \alpha x + \beta$ line (r^2), the root mean square error (RMSE) and model
237 efficiency (ME, *Nash and Sutcliffe*, 1970):

238 $$\text{RMSE} = \sqrt{\frac{1}{n}\sum_{i=1}^{n}(P_i - O_i)^2} \quad (1)$$

239 and

240

241 $$ME = 1 - \frac{\sum_{i=1}^{n}(P_i - O_i)^2}{\sum_{i=1}^{n}(O_i - O_{avg})^2} \quad (2)$$

242

243 where O_i is the *i*th observed value, P_i is the *i*th simulated value, O_{avg} is the average value of the
244 observations and *n* is the total number of data pairs. The RMSE values indicate the extent to which the
245 simulations are overestimating or underestimating observed values. ME represents the degree to
246 which variations in measured values are accounted by the model.

247 (17) After validation, the WAVES model was run with historical climate data (1981–2012) to
248 assess effects of climate variability on vegetation growth, water use and the corresponding controls on
249 deep drainage, below 4 m of the soil profile, which hereafter is referred to as recharge. During years
250 when ET represented less than 100% of annual precipitation, the remainder of the water budget deficit

drained below the bottom of the model (4 m) because runoff is only local in Mulga woodlands on very flat terrain, such as at this site (0.2%; *Cleverly et al.*, 2013a; *Eamus et al.*, 2013). The parameter values of vegetation (Mulga and understory), soil and initial conditions for model calibration were used. The simulations were undertaken for both the Mulga and understory. The 32 years of historical climate data were obtained from the nearest meteorological station, Territory Grape Farm (http://www.bom.gov.au) and were extracted from SILO (*Jeffrey et al.*, 2001), an enhanced climate database hosted by the Queensland Climate Change Centre of Excellence.

3. Results and Discussion

3.1. Model calibration and validation

(18) The performance of the WAVES model was evaluated by comparing simulated LAI, soil water content and ET (Figure 2−5). Although knowledge of LAI is vital to any mechanistic understanding of the hydrological role of vegetation (*Eamus et al.*, 2006), it is difficult to measure across large spatial scales and difficult to simulate due to spatial and temporal variability. To assess model performance, the simulated total LAI (over storey plus understory) was compared to field assessment of LAI (7 measurement campaigns) and MODIS LAI (Figure 2). In general, simulations of total LAI followed the seasonal patterns of both observed total LAI and MODIS LAI well (Figure 1a). MODIS derived landscape LAI generally ranged between 0.22 and 0.90 during the study period, with a single peak value between late February and early March for each year (0.90 in 2011 and 0.51 in 2012). Simulated total LAI ranged between 0.24 and 0.75 and reached a single peak between late February and early March (0.75 in 2011 and 0.48 in 2012), which was comparable to MODIS trends and ranges. The model was able to explain about 54% of the variation in MODIS LAI (0.10 RMSE) (Table 3).

(19) Good agreement was also obtained between simulated LAI of the canopy and understory and the corresponding LAI field observations (Figure 2b, c). The model explained about 93% of the variation in observed understory LAI (0.04 RMSE). An abrupt decrease in observed canopy LAI occurred in late January 2011, even with the receipt of substantial precipitation (Figure 2, 3), possibly

because of measurement error. When this single value was excluded, the overall performance of the model in simulating canopy LAI explained 65% of its variation (0.05 RMSE, Table 3). In this simulation, LAI was optimised to maintain a match between modelled and measured values of ET, resulting in a smaller r^2 with canopy LAI than in the understorey (Table 3) due to extreme variability in leaf physiology, water status and responses to moisture and heat stress of Mulga as a "stress endurer" (*Winkworth*, 1973; *O'Grady et al.*, 2009; *Cleverly et al.*, 2013a; *Eamus et al.*, 2013). Without considering natural variability in physiological parameters, the values of ME for both understory and canopy LAI were close to 1 (Table 3), thus indicating that the slope of the relationship between measured and modelled LAI was close to 1:1 (*Whitley et al.*, 2013).

(20) In general, soil water content (10- and 60-cm depths) and ET were simulated very well, although there were notable periods when the model did not match the measurements (Figures. 4, 5). The model was able to explain about 70% of the variation in soil water content (0.03 m^{-3} m^{-3} RMSE) during the experimental period (Table 3). Likewise, the model explained about 96% of the variation in cumulative ET with an RMSE of 1.07 mm d^{-1} (Table 3). Most importantly, ET and soil moisture content were largest in the summer, smallest in the winter, and followed a pulse-response pattern regardless of season (cf. Figures. 3, 4, 5). These results are consistent with a previous study at this site, wherein ET responded with a large, rapid increase after rainfall pulses larger than 2.5 mm, which was followed immediately by exponentially declining ET (*Eamus et al.*, 2013). However, the model used in this study tended to overestimate the magnitude of soil water content responses to rainfall, particularly when precipitation was very high (October 2010 to January 2011, cf. Figures. 3, 4). Failure to account for areas of restricted infiltration due to the occurrence of a spatially heterogeneous hardpan at this site (*Cleverly et al.*, 2013a) would lead to anomalies in modelled soil moisture profiles. In contrast, daily values of measured ET (0–5.9 mm) were marginally larger than simulated values (0–5.1 mm). Notwithstanding differences between simulated values and measurements, the model matched measurements of ET and soil water content very well, which was indicated by values of ME that were close to 1 (Table 3).

(21) We conclude from these results that the calibrated WAVES model is effective at simulating the responses of vegetation water-use and recharge in the study area, particularly with the climate variability in the region (*Cleverly et al.*, 2013a; *Papalexiou and Koutsoyiannis*, 2013). Previous applications of WAVES include ecohydrological examinations of climate, vegetation water balances (*Zhang et al.*, 1999a, b; *Wang et al.*, 2001; *Yang et al.*, 2003). Thus, WAVES was found to provide a reliable framework for evaluating ecohydrological responses of soil and vegetation to large-scale variations in climate.

3.2. Climate variations from 1981 to 2012

(22) Climate in the last 30 years (1981–2012) varied with large fluctuations in precipitation (97–833 mm yr^{-1}; Figure 6). Variations in mean annual mean temperature (21.2–23.4 ^{o}C), solar radiation (20.7–23.1 MJ m^{-2} d^{-1}) and VPD (1.3–2.1 kPa) were uniformly low during years when precipitation was large (Figure 6). The large variation in annual precipitation supply is typical of central Australia, where two types of storm systems generate moisture: the Australian low and the monsoon depression (*Kong and Zhao*, 2010; *Berry et al.*, 2011). The probability of receiving precipitation from either storm system is small (*Berry et al.*, 2011), which was shown in the years when annual rainfall was less than 100 mm (Figure 6). However, when both types of storm systems occur simultaneously, extraordinarily large amounts of precipitation can be received (*Kong and Zhao*, 2010), thereby causing the eight-fold range in rainfall shown in Figure 6. The negative temporal correlation of precipitation against radiation, temperature and VPD was indicative the ameliorating effects of cloudiness, rainfall and evaporative cooling on summer temperature regimes (*Cleverly et al.*, 2013a). Interestingly, a decreasing trend was seen since 2000 although the precipitation in 2010 was extremely high.

(23) Figure 7 shows the large monthly variability in climatic conditions. Monthly mean temperature and solar radiation were highly seasonal: temperature ranged between 13.6 and 29.8 ^{o}C in July and January, respectively (Figure 7a), while solar radiation ranged from 15.9 to 26.2 MJ m^{-2} over

331 the same period (July to January; Figure 7b). Precipitation was also highly seasonal, with more than
332 50% of precipitation falling in the three summer months (wet season, December to February) and
333 more than 80% falling during the monsoon season (November through April; Figure 7c). Interestingly,
334 VPD in the wet season was almost three times larger than in the dry season (June to August) (Figure
335 7d) due to high temperatures that compensated for the large absolute humidity during the summer. In
336 contrast, VPD in the tropical savannas of northern Australia are smaller in the wet season than during
337 the dry season, even though the range of mean monthly VPD values are similar in both locations (cf.
338 Figure 7 and *Whitley et al.*, 2011). The continental climate at this site is characterised by a distinct
339 summer wet season, a large difference between winter and summer temperatures, and the large values
340 of insolation that occur in tropical semi-arid regions (Figure 7), where the occurrence of cloud-free
341 conditions is common even during the wet season (*Cleverly et al.*, 2013a).
342
343 **3.3. Vegetation growth affected by climate variability**
344 (24) Figure 8 illustrates inter-annual variations in simulated annual mean LAI of the canopy and
345 understory during 1981–2012. Due to large inter-annual climate variability (Figure 6), simulated LAI
346 of both the canopy and understory also displayed large inter-annual variations. Simulated LAI of the
347 canopy ranged from 0.12 to 0.35 with an average of 0.25, while that of the understory ranged from
348 0.07 to 0.21 with an average of 0.13. Interestingly, an obvious decreasing trend was shown in
349 simulated understory LAI (Figure 8), reflecting the effect of the extended recent drought (Figure 6).
350 Due to strong seasonal variation in climate, especially precipitation and temperature (Figure 7),
351 seasonal variation in simulated understory LAI was large, ranging from 0.03 in September to a
352 maximum of 0.36 in February (Figure 9a). In contrast, simulated tree canopy LAI showed only a
353 small range in seasonal variation (0.22−0.28), reflecting the evergreen drought- and heat-tolerant
354 sclerophyllous nature of *Acacia* phyllodes (*Eamus et al.*, 2013). The "bulge" in the simulated
355 understory LAI from November through March (Figure 9a) coincided with the wet season (Figure 7c)
356 and reflects the precipitation dependent understory of forbs, shrubs and grasses, the latter of which are
357 comprised of species using the C_3 and C_4 photosynthetic pathways (*Cleverly et al.*, 2013b). These

responses of the understory to rainfall predominantly determine the intra-annual variation in total LAI (Figure 9a), as has been noted recently in a field study of this site (*Eamus et al.*, 2013).

(25) The different responses of the tree canopy and understory LAI to climate variations illustrates that the growth of Mulga and understory is responsive to different driving factors. At the inter- and intra-annual scales, variations in simulated LAI of the *Acacia* were equally uncorrelated to temperature, solar radiation, precipitation and VPD, with no single factor showing a significant correlation coefficient (Table 4). In contrast, understory LAI responded positively to smaller VPD and lower temperature at the intra-annual time scale (Table 4). These negative correlations at the inter-annual time scale are indicative of the negative correlation between temperature and precipitation at this site (section 3.2). In contrast, intra-annual variation in understory LAI were positively and significantly correlated to temperature and precipitation (Table 4), For the understory, monsoon-season precipitation was the most important factor driving variation in LAI, in agreement with extensive analyses by *Ma et al.* (2013), who compared phenological patterns along the 1100 km North Australian Tropical Transect.

3.4. Vegetation and climate interactions: vegetation water-use controls recharge

(26) Simulated vegetation water-use displayed strong seasonal variations (Figure 9b), as recently observed in eddy covariance data for this site (*Eamus et al.*, 2013). In Mulga, the largest rate of water-use occurred during early summer (December and January), reflecting the influence of summer rainfall, high temperature and large VPD in these months (Figure 7). In the understory, the largest rates of water use occurred in late summer (February) reflecting summer rainfall, high temperatures, large VPD and the increases in understory LAI that occurred throughout the summer (Figure 9a). These simulations demonstrate (a) that the major drivers of seasonal changes in vegetation water-use are different for the understory and overstory; and (b) the importance of vegetation dynamics in controlling the partitioning of water fluxes between ET and recharge in this arid region.

(27) Reliable estimates of vegetation water-use and recharge are critical for evaluation and optimal management of water resources. The importance of climate and vegetation in controlling the

components of the water cycle at this Mulga site is shown by the simulations of vegetation water-use and groundwater recharge as a function of climate for the period 1981–2012 (Figures 9 and 10). Annual water-use showed large year-to-year variability for both Mulga and understory; varying from 54 to 584 mm for the Mulga and from 3 to 35 mm for the understory. Mean annual water-use by the Mulga and understory was 232 and 19 mm, respectively (Figure 10). Total annual water-use by vegetation ranged from 64 to 601 mm, representing 44 to 100% of annual precipitation (Figures 6c and 10).

(28) Figure 11 shows the simulated annual recharge, with and without vegetation, at the Mulga site during 1981−2012. Annual recharge varied greatly and ranged from 0 to 48 mm, with an average of 6 mm, representing 1.8% of precipitation on average. Due to large climate variability, the simulated values of recharge without vegetation effects ranged from 58 to 672 mm with an average of 236 mm. This accounted for 18–100% of annual precipitation, highlighting the importance of vegetation for controlling recharge. Moreover, the difference in annual recharge between simulations that did and did not include the presence of vegetation was much smaller in dry years than in wet years (data not shown), which indicates the ability of vegetation to reduce recharge in water-limited environments. These values assume that permeability of the soil is equivalent in vegetated and un-vegetated patches. However, bare soil patches are common in Mulga as surface expressions of an impermeable hardpan (*Cleverly et al.*, 2013a) from which local redistribution of rainfall creates run-on zones beneath the vegetation (*Dunkerley and Brown*, 1995; *Ludwig et al.*, 2005).

(29) There was almost no recharge when annual precipitation was less than 400 mm, which is nearly 100 mm above average (306 mm; http://www.bom.gov.au), and very little recharge (less than 6 mm, annual mean average) occurred in almost 70% of years (Figure 12a). However, large variations in rates of recharge occurred for different years that had similar total annual rainfall. For example, there was about 47.6 mm of recharge in 2001 when annual rainfall was 470.9 mm (circled with open circle; Figure 12a) but there was no recharge in 1991 when rainfall was 458.7 mm (circled in Fig 12a). This large difference in recharge despite similar annual rainfall is likely to be because of the effect of carry-over of soil water from one year to the next. In 2000, there was about 743.3 mm of rainfall

412 (Figure 6c), which exceeded water demand by vegetation and thus excess rainfall was stored in the
413 soil and in the following year rain was received by a wet soil profile and this "pushed" recharge to
414 deeper layers. In contrast, in 1990, there was only 221.0 mm which, was almost entirely used by
415 vegetation (Figure 10). As a result, rain in 1991 was received by a much drier soil profile and water
416 not used by vegetation was stored in the soil instead of generating recharge. Such a carry-over effect
417 has previously been demonstrated in semi-arid grasslands and woodlands (Flanagan et al., 2011; Raz-
418 Yaseef et al., 2012). Furthermore, due to the rapid response of Mulga to precipitation, rainfall
419 intensity does not show significant effects on recharge (Figure 12b). The coefficient of variation (CV)
420 of simulated annual recharge was 1.67, much larger than that of annual precipitation (CV = 0.47).
421 This indicates that annual recharge was more variable than annual precipitation and this is most likely
422 due to water-use by vegetation. The simulated recharge showed little seasonal variations due to low
423 values as a result of precipitation used by vegetation (Figure 13).

424 (30) Simulated recharge was significantly affected by all climatic variables (temperature, solar
425 radiation, rainfall, rainfall intensity and VPD) (Table 4). This occurs because all of these factors,
426 singly and in combination, determine (a) rates of ET at daily and seasonal scales (*Whitley et al.*, 2009);
427 (b) seasonal patterns in LAI (*Ma et al.*, 2013); and (c) from the interaction of (a) and (b), partitioning
428 of rainfall into transpiration, soil evaporation and deep drainage (Figures 8, 10, 11).

429 (31) Absolute values of fluxes estimated by our model are subject to some uncertainty, although the
430 temporal patterns which are of primary interest in this paper are likely to be reliable. In particular,
431 previous studies in the Ti-Tree Basin have estimated spatially and temporally averaged recharge of
432 approximately 2 mm/yr, although much of this might occur as infiltration through ephemeral streams
433 with negligible recharge across other areas of the basin (*Harrington et al.*, 2002). Uncertainties in
434 model predictions arise due to errors in model parameters and due to simplifications inherent in the
435 way that the model represents the hydrological system (often termed structural errors). In this study,
436 drainage below 4 m has been equated with recharge, although the rooting depth of mulga remains
437 somewhat uncertain. If it is deeper than 4 m, then a lower mean recharge flux would be calculated
438 (data not shown). The absolute values of recharge will also be sensitive to soil hydraulic parameters.

Although these are able to be partially determined through calibration to observed water content data, water content data are not available below 1.2 m, and this also introduces some uncertainty in the drainage rate. Precipitation has been measured with a tipping-bucket raingauge, which has some local random errors in precipitation measurements (*Ciach*, 2003) and arid zone precipitation is also highly spatially variable (*Lemos et al.*, 2002). This will also affect the absolute value of drainage.

(32) Our results demonstrate that climate-vegetation interactions exert strong controls on rates of recharge through their impact on LAI and hence vegetation water-use. Knowledge of the interactions amongst all three factors and their controls on groundwater recharge can be used to assess potential impacts of climate variability and land use/land cover change on vegetation health and groundwater availability and has a regional application to management of groundwater resources. Our analyses did not show obvious relationship between modelled recharge and rainfall amount and rainfall intensity (Figure 12). Inter-annual variability in rainfall is magnified 2- to 4-times in variability in modelled recharge. This indicates that, for an adequate water resources assessment, there is a need to account for the effects of historical variability in climatic conditions and vegetation dynamics on renewable groundwater resources. As the effect of vegetation on groundwater recharge is significant (Figure 11), it is likely that if land use was to change significantly in response to climate change, the indirect effect of climate change on recharge may be larger than changes in rainfall or temperature. Thus, understanding vegetation response to inter-annual variability of climate should be central in any attempt to predict hydrologic change (*Troch et al.*, 2009).

4. Conclusions

(33) To allocate groundwater resources optimally it is important to consider both the water requriement of vegetation and the interaction of vegetation structure and function and their interactions with climate. Physically-based ecohydrological models are useful tools that can be used to investigate responses of vegetation and the components of a site's water balance to climate variability. In this study, a biophysically based model, WAVES, was applied to examine physiological

and hydrological responses of vegetation to climate variations in an arid zone landscape dominated by an *Acacia* (Mulga) savanna woodland. We found that:

- The WAVES model was able to reasonably reproduce the dynamics of vegetation growth, vegetation water-use and changes in soil water content in this arid zone landscape. Thus we can use WAVES to investigate the interactions between climate and vegetation and the components of the site's water balance.
- Simulated annual mean LAI ranged from 0.12 to 0.35 for the overstory canopy and 0.07 to 0.21 for the understory, as a result of large inter-annual climatic variability, especially precipitation.
- From the model simulations with long-term climate data we showed that climate variability greatly affected vegetation water-use and hence groundwater recharge. Simulated annual water-use by vegetation (Mulga & understory) ranged from 64 to 601 mm. The largest rate of vegetation water use was due to high temperature and adequate precipitation in summer months (December to February). Annual recharge when vegetation was excluded from the simulations was highly variable and this variability was mostly dependent on variation in inter-annual precipitation, which ranged from 58 to 672 mm.
- Comparsion of recharge between with and without vegetation effects indicated that vegetation exerted strong controls on recharge, which was simulated to reduce recharge by 54 to 653 mm per year. Relative reductions in recharge due to vegetation were larger in dry years than wet years, reflecting the enhanced ability of vegetation to reduce recharge in water-limited environments.

(33) The results give an insight into assessing potential impacts of climate variability and land use/land cover change on groundwater resources management.

Acknowledgements.

(34) This work was supported by grants from National Centre for Groundwater Research and Training (NCGRT) and the Australian Government's Terrestrial Ecosystems Research Network (TERN) (www.tern.gov.au). This work was supported also by OzFlux and the Australian Supersite Network, both parts of TERN and the latter of which is a research infrastructure facility established under the

National Collaborative Research Infrastructure Strategy and Education Infrastructure Fund–Super Science Initiative, through the Department of Industry, Innovation, Science, Research and Tertiary Education. We are grateful to Professor Qiang Yu for his useful suggestions.

References

Anderson, L., van Klinken, R. D., and Shepherd, D. (2008). Aerially surveying Mesquite (Prosopis spp.) in the Pilbara. In: 'A Climate of Change in the Rangelands. Proceedings of the 15th Australian Rangeland Society Biennial Conference'. (Ed. D. Orr) 4 pages. (Australian Rangeland Society: Australia).

Baird, K. J., J. C. Stromberg, and III. T. Maddock (2005), Linking riparian dynamics and groundwater: an ecohydrologic approach to modeling groundwater and riparian vegetation, *Environ. Manage.*, *36*, 551–564.

Ball, J. T. (1987), Int. Congress 7th. Prog. Photosynthesis Res. Proc., *Providence*, 10-15 Aug 1986, pp. 221–224.

Barr, A. G., A. K. Betts, T. A. Black, J. H. McCaughey, and C. D. Smith (2001), Intercomparison of BOREAS northern and southern study area surface fluxes in 1994, *J. Geophys. Res.*, *106*, 33543–33550.

Barr, A. G., G. van der Kamp, R. Schmidt, and T. A. Black (2000). Monitoring the moisture balance of a boreal aspen forest using a deep groundwater piezometer, *Agric. Forest Meteorol.*, 102, 13–24.

Barron, O. V., R. S. Crosbie, W. R. Dawes, S. P. Charles, T. Pickett, and M. J. Donn (2012), Climate controls on diffuse groundwater recharge across Australia, *Hydrol. Earth Syst. Sci.*, *16*, 4557–4570.

Berry, G., M. J. Reeder, and C. Jakob, 2011: Physical mechanisms regulating summertime rainfall over northwestern Australia, *J. Clim.*, *24*, 3705–3717.

Berry, S. L., G. D. Farquhar, and M. L. Roderick (2005), Co–Evolution of Climate, Soil and Vegetation, *Encyclopedia of hydrological sciences*.

Broadbridge, P., and I. White (1988) Constant rate rainfall infiltration: A versatile nonlinear model: 1. Analytic solution, *Water Res. Res., 24,* 145–154.

519 Chen, C., E. Wang, and Q. Yu (2010), Modelling the effects of climate variability and water
520 management on crop water productivity and water balance in the North China Plain, *Agric. Water*
521 *Manage.*, *97*, 1175–1184.
522 Ciach, G. J. (2003). Local random errors in tipping-bucket rain gauge measurements. *J. Atmos.*
523 *Oceanic Technol.*, *20*, 752–759.
524 Cleverly J., N. Boulain, R. Villalobos-Vega, N. Grant, R. Faux, C. Wood, P.G. Cook, Q. Yu, A. Leigh,
525 and D. Eamus (2013a), Dynamics of component carbon fluxes in a semi-arid Acacia woodland,
526 central Australia, *J. Geophys. Res.*, doi: 10.1002/jgrg.20101.
527 Cleverly, J. (2011), Alice Springs Mulga OzFlux site. OzFlux: Australian and New Zealand Flux
528 Research and Monitoring Network, hdl: 102.100.100/8697.
529 Cleverly, J., C. Chen, N. Boulain, R. Villalobos-Vega, R. Faux, N. Grant, Q. Yu, and D. Eamus
530 (2013b), Aerodynamic resistance and Penman-Monteith evapotranspiration over a seasonally two-
531 layered canopy in semi-arid central Australia, *J. Hydrometeor.*, doi: 10.1175/JHM-D-13-080.1.
532 Clifton, C., and R. Evans (2001), Environmental water requirements of groundwater dependent
533 ecosystems, *Environmental flows Initiative Technical Report*, Report, 2.
534 Constantin, J., M. G. Inclan, and M. Raschendorf (1998), The energy budget of a spmce forest: field
535 measurements and comparison with the forest-land-atmosphere model (FLAME), *J. Hydrol.*, *2*, 12-
536 213:2 2-35.
537 Crosbie, R. S., I. D. Jolly, F. W. Leaney, and C. Petheram (2010), Can the dataset of field based
538 recharge estimates in Australia be used to predict recharge in data-poor areas?, *Hydrol. Earth Syst.*
539 *Sci.*, *14*, 2023–2038, doi:10.5194/hess-14-2023-2010.
540 Crosbie, R.S., J. McCallum, G. R. Walker, and F. H. S. Chiew (2008), Diffuse groundwater recharge
541 modelling across the Murray-Darling Basin. A report to the Australian government from the CSIRO
542 Murray-Darling Basin Sustainable Yields project, Water for a Healthy Country Flagship, CSIRO,
543 Canberra, http://www.csiro.au/files/files/pn7z.pdf.

544 Crosbie, R.S., W. R. Dawes, S. P. Charles, F. S. Mpelasoka, S. Aryal, O. Barron, G. K. Summerell
545 (2011), Differences in future recharge estimates due to GCMs, downscaling methods and
546 hydrological models, *Geophys. Res. Lett., 38*, L11406.
547 Dawes, W. R., M. Gilfedder, M. Stauffacher, J. Coram, S. Hajkowicz, G. R. Walker, and M. Young
548 (2002), Assessing the viability of recharge reduction for dryland salinity control: Wanilla, Eyre
549 Peninsula. *Aust. J. Soil Res., 40*, 1407–1424.
550 Dawes, W., and T. J. Hatton (1993) Topog_IRM 1. Model description. CSIRO Division of Water
551 Resources, *Technical Memorandum, 93*, 33 p
552 Dawes, W.R., L. Zhang, and P. Dyce (1998), WAVES V3.5 User Manual, CSIRO Land and Water,
553 Canberra, ACT.
554 Donohue, R. J., M. L. Roderick, and T. R. McVicar (2007), On the importance of including
555 vegetation dynamics in Budyko's hydrological model(J), *Hydrol. Earth Syst. Sci. Discuss., 11*, 983–
556 995.
557 Dunkerley, D. L., and K. J. Brown (1995), Runoff and runon areas in a patterned chenopod shrubland,
558 arid western New South Wales, Australia – characteristics and origin, *J. Arid. Environ., 30*, 41–55.
559 Eamus, D. (2003), How does ecosystem water balance affect net primary productivity of woody
560 ecosystems?(J), *Funct. Plant Biol., 30*, 187–205.
561 Eamus, D., J. Cleverly, N. Boulain, N. Grant, R. Faux, and R. Villalobos-Vega (2013), Carbon and
562 water fluxes in an arid-zone *Acacia* savanna woodland: An analyses of seasonal patterns and
563 responses to rainfall events, *Agric. For. Meteor.*, http://dx.doi.org/10.1016/j.agrformet.2013.04.020.
564 Eamus, D., T. Hatton, P. Cook, and C. Colvin (2006), Ecohydrology: vegetation function, water and
565 resource management, *CSIRO Publishing*: Collingwood.
566 Flanagan, L.B., Adkinson, A.C., 2011. Interacting controls on productivity in a northern
567 Great Plains grassland and implications for response to ENSO events. Global Change
568 Biology, 17, 3293–3311.
569 Farrington, P., E. A. N. Greenwood, G. A. Bartle, J. D. Beresford, and G. D. Watson (1989),
570 Evaporation from *Banksia* woodland on a groundwater mound, *J. Hydrol., 105*, 173–186.

571 Fernandez, J. E., C. Slawinski, F. Moreno, R. T. Walczak, and M. Vanclooster (2002), Simulating the
572 fate of water in a soil–crop system of a semi-arid Mediterranean area with the WAVE 2.1 and the
573 EURO-ACCESS-II models, *Agric. water manage.*, *56*, 113–129.
574 Garcia, C.A., Andraski, B.J., Stonestrom, D.A., Cooper, C.A., Simunek, J., and Wheatcraft, S.W.,
575 2011, Interacting vegetative and thermal contributions to water movement in desert soil: Vadose
576 Zone Journal, v. 10, no. 2, p. 552-564, doi:10.2136/vzj2010.0023.
577 Gee, G.W., Wierenga, P.J., Andraski, B.J., Young, M.H., Fayer, M.J., and Rockhold, M.L., 1994,
578 Variations in water balance and recharge potential at three western desert sites: Soil Science Society
579 of America Journal, v. 58, no. 1, p. 63-72.
580 Guswa, A. J., M. A. Celia, I. Rodriguez-Iturbe (2002), Models of soil moisture dynamics in
581 ecohydrology: A comparative study, *Water Res. Res.*, *38*, 5-1–5-15.
582 Harrington, G., P. G. Cook, A. L. Herczeg (2002), Spatial and temporal variability of ground water
583 recharge in central Australia: a tracer approach, *Groundwater*, *40*, 518–528.
584 Hill, S. M., & Hill, L. J. (2003). Some important plant characteristics and assay overviews for
585 biogeochemical surveys in western New South Wales. *Advances in Regolith. CRC LEME*, 187-192.
586 Jeffrey, S. J., J. O. Carter, K. B. Moodie, and A. R. Beswick (2001), Using spatial interpolation to
587 construct a comprehensive archive of Australian climate data, *Environ. Modell. Softw.*, *16*, 309–330.
588 Jha, M., A. Chowdhury, V. Chowdary, and S. Peiffer (2007), Groundwater management and
589 development by integrated remote sensing and geographic information systems: prospects and
590 constraints, *Water Resour. Manage.*, *21*, 427–467
591 Johnston, R. M., S. J. Barry, E. Bleys, E. N. Bui, C. J. Moran, D. A. P. Simon, P. Carlile, N. J.
592 McKenzie, B. L. Henderson, G. Chapman, M. Imhoff, D. Maschmedt, D. Howe, C. Grose, N.
593 Schoknecht, B. Powell, and M. Grundy (2003), ASRIS: the database, *Aust. J. Soil. Res.*, *41*, 1021–
594 1036.
595 Kingston, D. G., and R. G. Taylor (2010), Sources of uncertainty in climate change impacts on river
596 discharge and groundwater in a headwater catchment of the Upper Nile Basin, Uganda, *Hydrol.*
597 *Earth Syst. Sci.*, 14, 1297–1308.

598 Kong, Q., S. Zhao (2010), Heavy rainfall caused by interactions between monsoon depression and
599 middle-latitude systems in Australia: a case study, *Meteorol. Atmos. Phys.*, *106*, 205–226, doi:
600 10.1007/s00703-010-0060-5.
601 Kucharik, C. J., J. A. Foley, C. Delire, V. A. Fisher, M. T. Coe, J. D. Lenters, C. Young-Molling, N.
602 Ramankutty, J. M. Normal, and S. T. Gower (2000), Testing the performance of a Dynamic Global
603 Ecosystem Model: water balance, carbon balance, and vegetation structure, *Global Biogeochem.*
604 *Cycles*, *14*, 795–825.
605 Laio, F., A. Porporato, L. Ridolfi, and Rodriguez-Iturebe (2001), Plants in water-controlled
606 ecosystems: Active role in hydrologic processes and response to water stress: II. Probabilistic soil
607 moisture dynamics, *Adv. Water Res.*, *24*, 707–723.
608 Lemos, M. C., T. J. Finan, R. W. Fox, D. R. Nelson, and J. Tucker (2002), The use of seasonal
609 climate forecasting in policymaking: lessons from Northeast Brazil. *Climatic Change*, *55*, 479-507.
610 Leuning, R. (1995), A critical appraisal of a combined stomatal–photosynthesis model for C3
611 plants(J), *Plant Cell Environ.*, *18*, 339–355.
612 Li, Z. Q., G. R. Yu, X. F. Wen, L. M. Zhang, C. Y. Re, and Y. L. Fu (2005), Energy balance closure
613 at ChinaFLUX sites, *Sci. China Ser. D-Earth Sci.*, *48*, 51–62.
614 Ludwig, J. A., B. P. Wilcox, D. D. Breshears, D. J. Tongway, and A. C. Imeson (2005), Vegetation
615 patches and runoff-erosion as interacting ecohydrological processes in semiarid landscapes,
616 *Ecology*, *86*, 288-297.
617 Ma, X., A. Huete, Q. Yu, N. Restrepo Coupe, K. Davies, M. Broich, P. Ratana, J. Beringer, L. B.
618 Hutley, J. Cleverly, N. Boulain, and D. Eamus (2013), Spatial patterns and temporal dynamics in
619 savanna vegetation phenology across the North Australian Tropical Transect, *Remote Sens.*
620 *Environ.*, *139*, 97-115, doi: 10.1016/j.rse.2013.07.030.
621 MacFarlane, C., M. Hoffman, D. Eamus, N. Kerp, S. Higginson, R. McMurtrie, and M. Adams
622 (2007), Estimation of leaf area index in eucalypt forest usingdigital photography, *Agric. For. Met.*,
623 *143*, 176–188, http://dx.doi.org/10.1016/j.agrformet.2006.10.013.

624 Martin, M., R. Silberstein, K. Smettem, and C. C. Xu (2008), Identifying Sources of Uncertainty in
625 Groundwater Recharge Estimates Using the Biophysical Model WAVES. In: Lambert, Martin
626 (Editor); Daniell, TM (Editor); Leonard, Michael (Editor). Proceedings of Water Down Under.
627 Modbury, SA: Engineers Australia; Causal Productions, 2161–2169.
628 McNaughton, K. G., and P. G. Jarvis (1991), Effects of spatial scale on stomatal control of
629 transpiration, *Agric. Forest Meteorol.*, *54*, 279–302.
630 Monteith, J., and M. Unsworth (2008), Principles of Environmental Physics, Edward Arnold, London,
631 UK, 250 pp.
632 Morton, S. R., D. M. S. Smith, C. R. Dickman, D. L. Dunkerley, M. H. Friedel, R. R. J. McAllister, J.
633 R. W. Reid, D. A. Roshier, M. A. Smith, F. J. Walsh, G. M. Wardle, I. W. Watson, and M. Westoby,
634 (2011), A fresh framework for the ecology of arid Australia, *J. Arid Environ.*, *75*, 313–329,
635 http://dx.doi.org/10.1016/j.jaridenv.2010.11.001.
636 Nash, J. E., J. V. Sutcliffe (1970), River flow forecasting through conceptual models part I–A
637 discussion of principles, *J. hydrol.*, *10*, 282–290.
638 O'Grady, A. P. P. G. Cook, D. Eamus, A. Duguid, J. D. H Wischusen, T. Fass, D. Worldege (2009),
639 Convergence of tree water use within an arid-zone woodland, *Oecologia*, *160*, 643–655, doi:
640 10.1007/s00442-009-1332-y.
641 Papalexiou, S. M. , and D. Koutsoyiannis (2013), Battle of extreme value distributions: A global
642 survey on extreme daily rainfall, *Water Resour. Res.*, *49*, doi: 10.1029/2012wr012557.
643 Porporato, A., P. D'odorico, F. Laio, L. Ridolfl, and I. Rodriguez-lturbe (2002), Ecohydrology of
644 water-controlled ecosystems, Adv. Water Res., 25, 1335–1348.
645 Raz-Yaseef, N., Yakir, D., Schiller, G., Cohen, S., 2012. Dynamics of evapotranspiration partitioning
646 in a semi-arid forest as affected by temporal rainfall patterns. Agricultural and Forest Meteorology
647 157, 77–85.
648 Ritchie, J. T., J. R. Kiniry, C. A. Jones, and P. T. Dyke (1986), Model inputs. In C. A. Jones and J. R.
649 Kiniry (Editors), CERES-Maize: a Simulation Model of Maize Growth and Development, Texas
650 A&M University Press, College Station, pp. 37–48.

651 Scanlon, B.R., Levitt, D.G., Reedy, R.C., Keese, K.E., and Sully, M.J., 2005, Ecological controls on
652 water-cycle response to climate variability in deserts: Proceedings of the National Academy of
653 Sciences of the United States of America, v. 102, no. 17, p. 6033-6038,
654 doi:10.1073/pnas.0408571102.
655 Sellers, P. J., J. A. Berry, G. J. Collatz, C. B. Field, and F. G. Hall (1992), Canopy reflectance,
656 photosynthesis, and transpiration. III. A reanalysis using improved leaf models and a new canopy
657 integration scheme, *Remote Sens. Environ., 42*, 187–216.
658 Singh, S., J. G. Kroes, J. C. van Dam, R. A. Feddes (2006), Distributed ecohydrological modelling to
659 evaluate the performance of irrigation system in Sirsa district, India: I. Current water management
660 and its productivity, *J. Hydrol.,* 329, 692–713.
661 Thorburn, P. J., T. J. Hatton, and G. R. Walker (1993), Combining measurements of transpiration and
662 stable isotopes of water to determine groundwater discharge from forests, *J. Hydrol., 150*, 563–587.
663 Troch, P. A., G. F. Martinez, V. R. N Pauwels, M. Durcik, M. Sivapalan, C. J. Harman, P. D. Brooks,
664 H. V. Gupta, and T. E. Huxman (2009), Climate and vegetation water use efficiency at catchment
665 scales, *Hydrol. Processes*, *23*, 2409–2414.
666 Twine, T. E., W. P. Kustas, J. M. Norman, D. R. Cook, P. R. Houser, T. P. Meyers, J. H. Prueger, P. J.
667 Starks, and M. L. Wesely (2000), Correcting eddy-covariance flux underestimates over a grassland,
668 *Agric. For. Meteorol., 103*, 279–300.
669 Wang, H. X., L. Zhang, W. R. Dawes, and C. M. Liu (2001), Improving water use efficiency of
670 irrigated crops in the North China Plain–measurements and modelling, *Agric. Water Manage., 48*,
671 151–167.
672 Whitley, R. J, C. M. O. Macinnis-Ng, L. B. Hutley, J. Beringer, M. Zeppel, M. Williams, D. Taylor,
673 D. Eamus (2011), Is productivity of mesic savannas light limited or water limited? Results of a
674 simulation study, *Glob. Change Biol., 17*, 3130–3149, doi: 10.1111/j.1365-2486.2011.02425.x.
675 Whitley, R. J., B. E. Medlyn, M. J. B. Zeppel, C. M. O. Macinnis-Ng, D. Eamus (2009), Comparing
676 the Penman–Monteith equation and a modified Jarvis–Stewart model with an artificial neural
677 network to estimate stand scale transpiration and canopy conductance. *J. Hydrol.,* 373, 256–266.

678 Whitley, R. J., D. Taylor, C. Macinnis-Ng, M. Zeppel, I. Yunusa, A. O'Grady, R. Froend, B. Medlyn,
679 D. Eamus (2013), Developing an empirical model of canopy water flux describing the common
680 response of transpiration to solar radiation and VPD across five contrasting woodlands and forests,
681 *Hydrol. Process.*, *27*, 1133-1146, doi: 10.1002/hyp.9280.
682 Wilson, K., et al. (2002), Energy Balance Closure at FLUXNET Sites, *Agric. For. Meteorol., 113*,
683 223–243.
684 Winkworth, R. E. (1973), Eco-physiology of Mulga (*Acacia aneura*), *Tropical Grasslands*, *7*, 43–48.
685 Wu, H., E. J. Rykiel Jr, T. Hatton, and J. Walker (1994), An integrated rate methodology (IRM) for
686 multi-factor growth rate modelling, *Ecolo. Model., 73*, 97–116.
687 Yang, Y., M. Watanabe, Z. Wang, Y. Sakura, and C. Tang (2003), Prediction of changes in soil
688 moisture associated with climatic changes and their implications for vegetation changes: Waves
689 model simulation on Taihang Mountain, China, *Clim. Change, 57*, 163–183.
690 Zhang, L., I. H. Hume, M. G. O'Connell, D. C. Mitchell, P. L. Mithorepe, M. Yee, W. R. Dawes, T. J.
691 Hatton (1999b), Estimating episodic recharge under different crop/pasture rotations in the Mallee
692 region. Part 1. Experiments and model calibration, *Agric. Water Manage., 42*, 219–235.
693 Zhang, L., W. R. Dawes (Eds.) (1998), WAVES—An Integrated Energy and Water Balance Model.
694 Technical Report No. 31/98, CSIRO Land and Water, Canberra, Australia.
695 Zhang, L., W. R. Dawes, P. G. Slavich, W. S. Meyer, P. J. Thorburn, D. J. Smith, G. R. Walker
696 (1999a), Growth and ground water uptake responses of lucerne to changes in groundwater levels
697 and salinity: lysimeter, isotope and modelling studies, *Agric. Water Manage., 39*, 265–282.
698 Zhang, L., W. R. Dawes, T. J. Hatton (1996), Modelling hydrologic processes using a biophysically
699 based model—application of WAVES to FIFE and HAPEX-MOBILHY, *J. Hydrol., 185*, 147–169.
700 Zhang, Y., K. E. Schilling (2006), Effects of land cover on water table, soil moisture,
701 evapotranspiration, and groundwater recharge: a field observation and analysis, *J. Hydrol., 319*,
702 328–338.

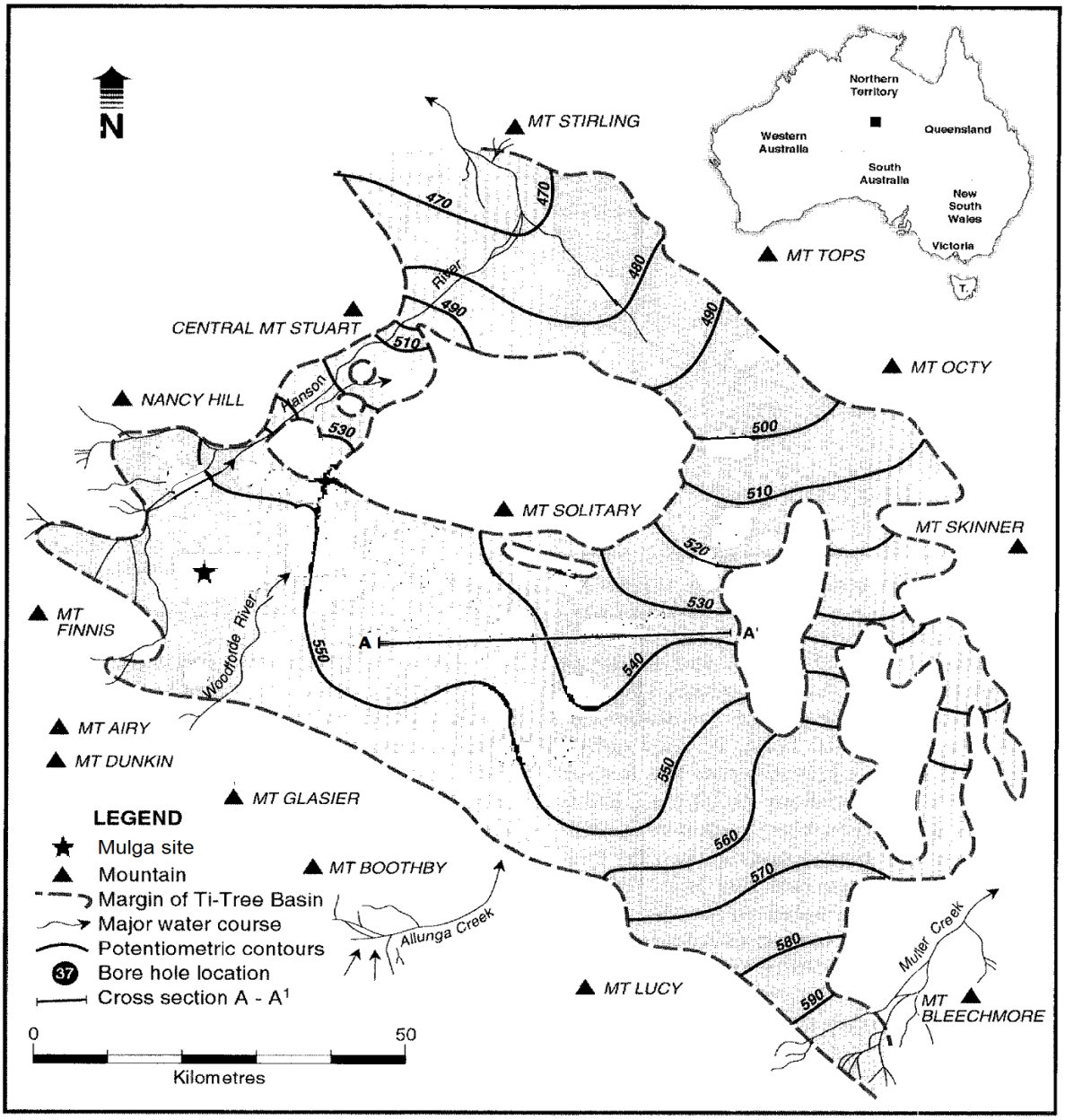

703

704 **Figure 1.** The Ti-Tree Basin, central Australia (small black square on inset map) and the study site

705 (Modified from Harrington et al., (2002)). Potentiometric contours indicate the general direction of

706 groundwater flow is to the east and north from the western and southern margins, respectively.

707

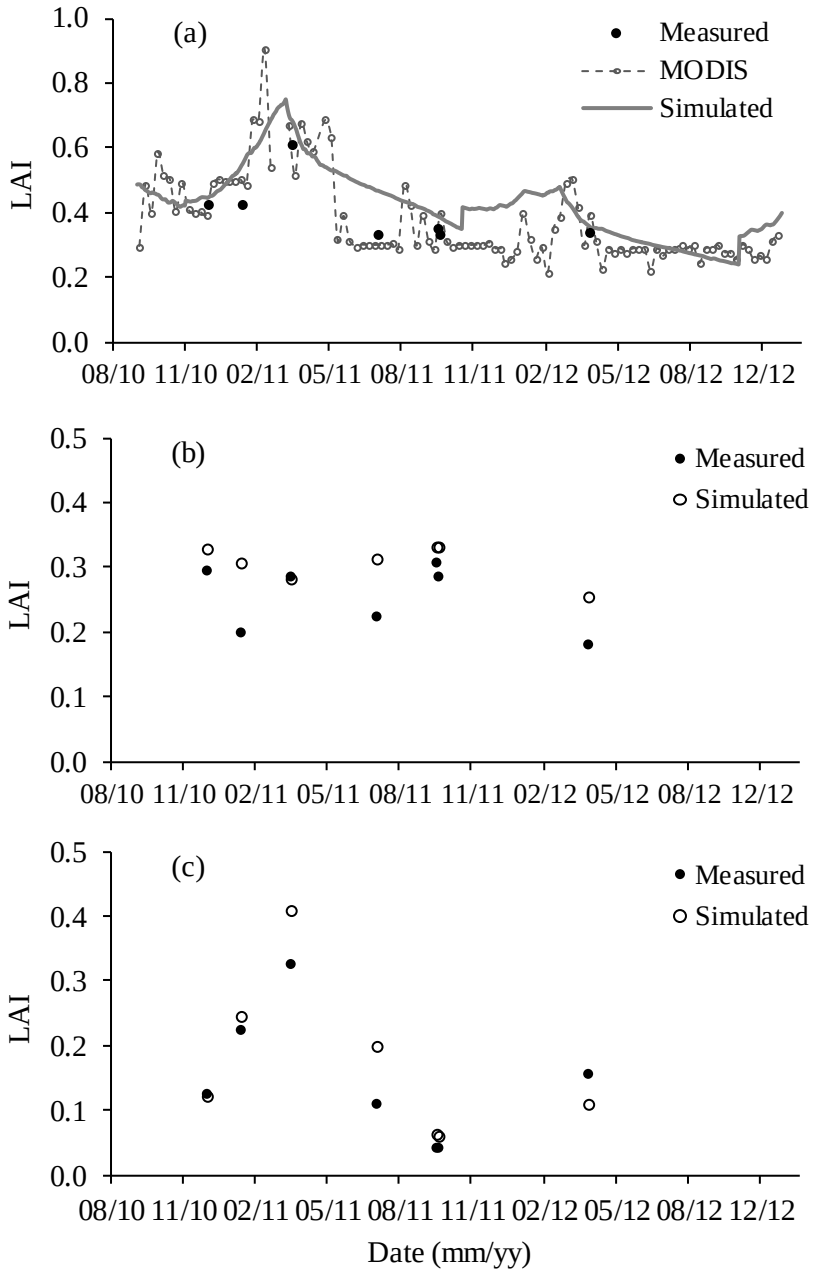

708

709 **Figure 2.** Comparison of total leaf area index (LAI) from digital photography (measured),
710 MODIS and that of simulations (a). Comparison of measured and simulated component
711 contributions of canopy (b) and understory (c) LAI from 3 September 2010 to 9 May 2012.

712

713

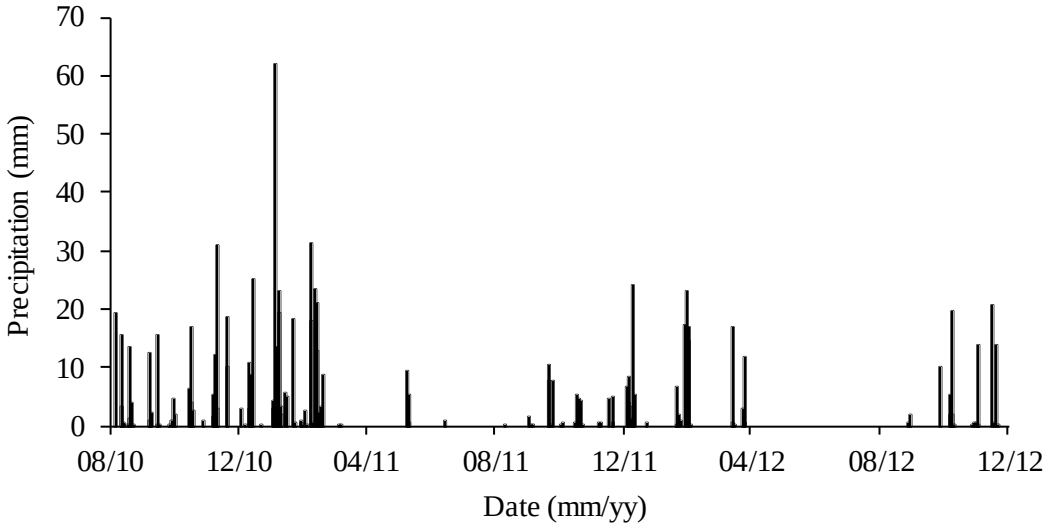

714

715 **Figure 3.** Daily precipitation measured at the study site during September 2010−December 2012.

716

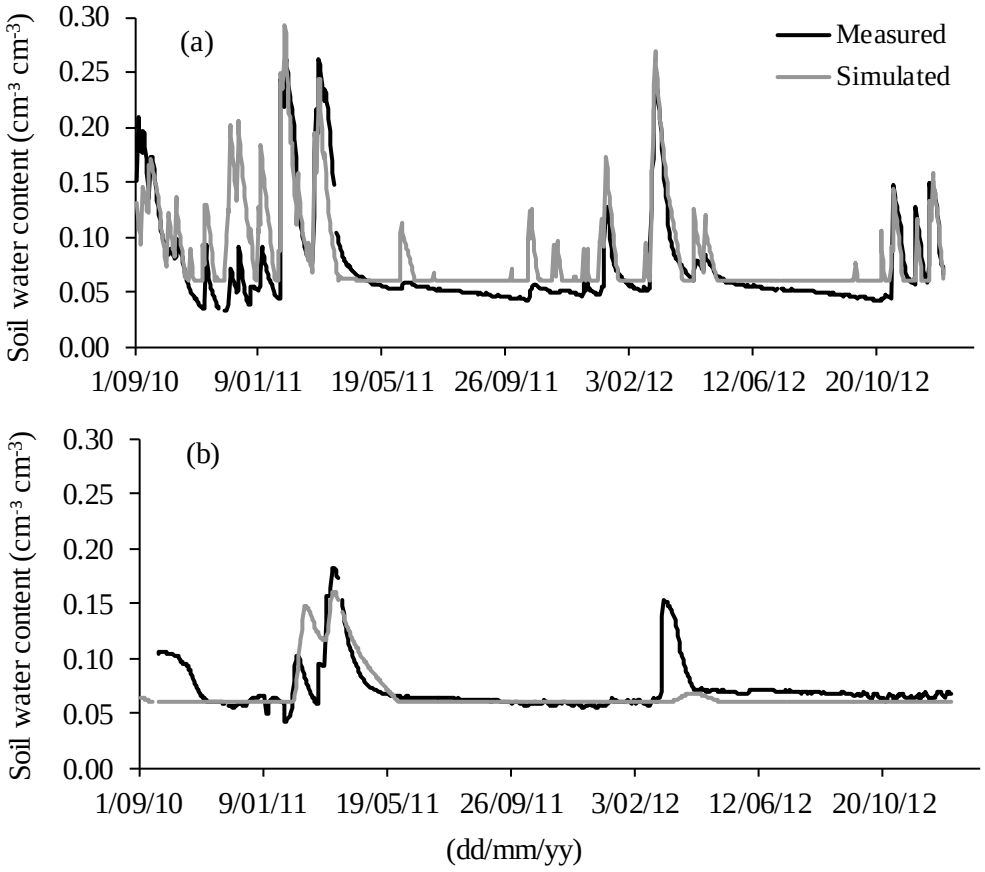

717

718 **Figure 4.** Comparison of measured and simulated soil water content at 10 cm (a) and 60 cm (b)

719 depths from 1 Sep 2010 to 31 December 2012.

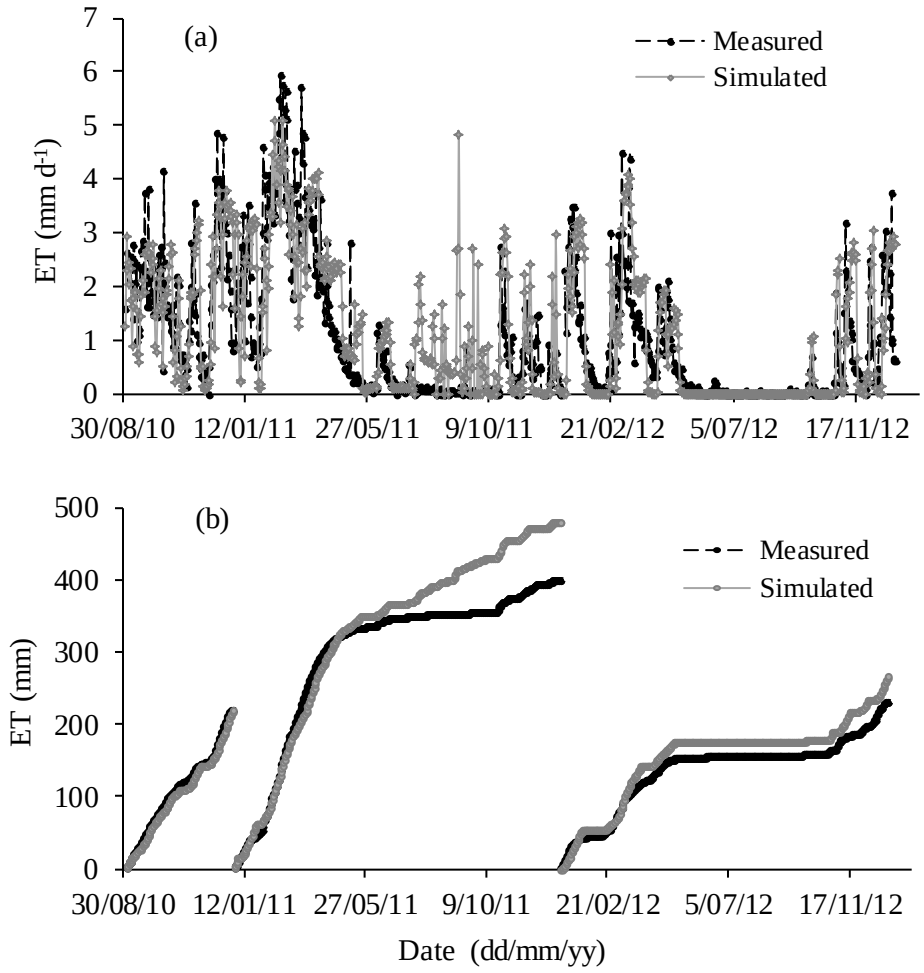

720

721 **Figure 5.** Comparison of measured and simulated daily ET (a) and cumulative ET (b) at Alice Spring

722 flux station from 3 September 2010 to 31 December 2012.

723

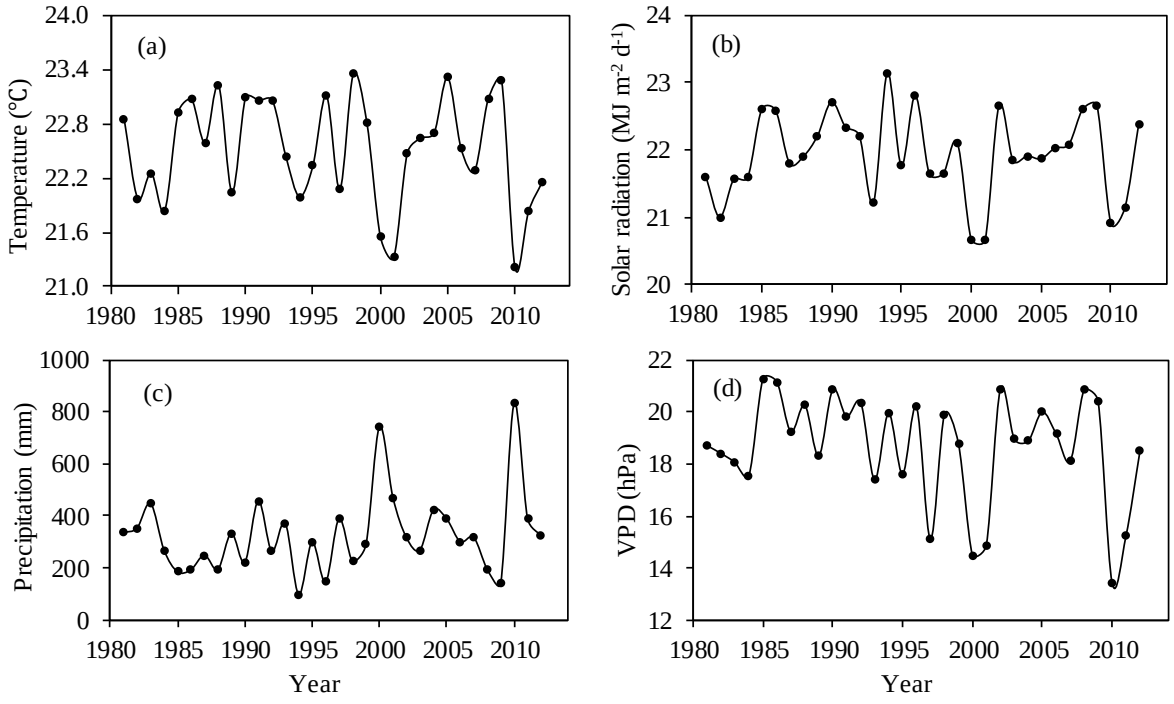

724

725 **Figure 6.** Annual mean temperature (a), annual mean solar radiation (b), annual precipitation (c) and

726 annual mean vapour pressure deficit (VPD) (d) during 1981–2012.

727

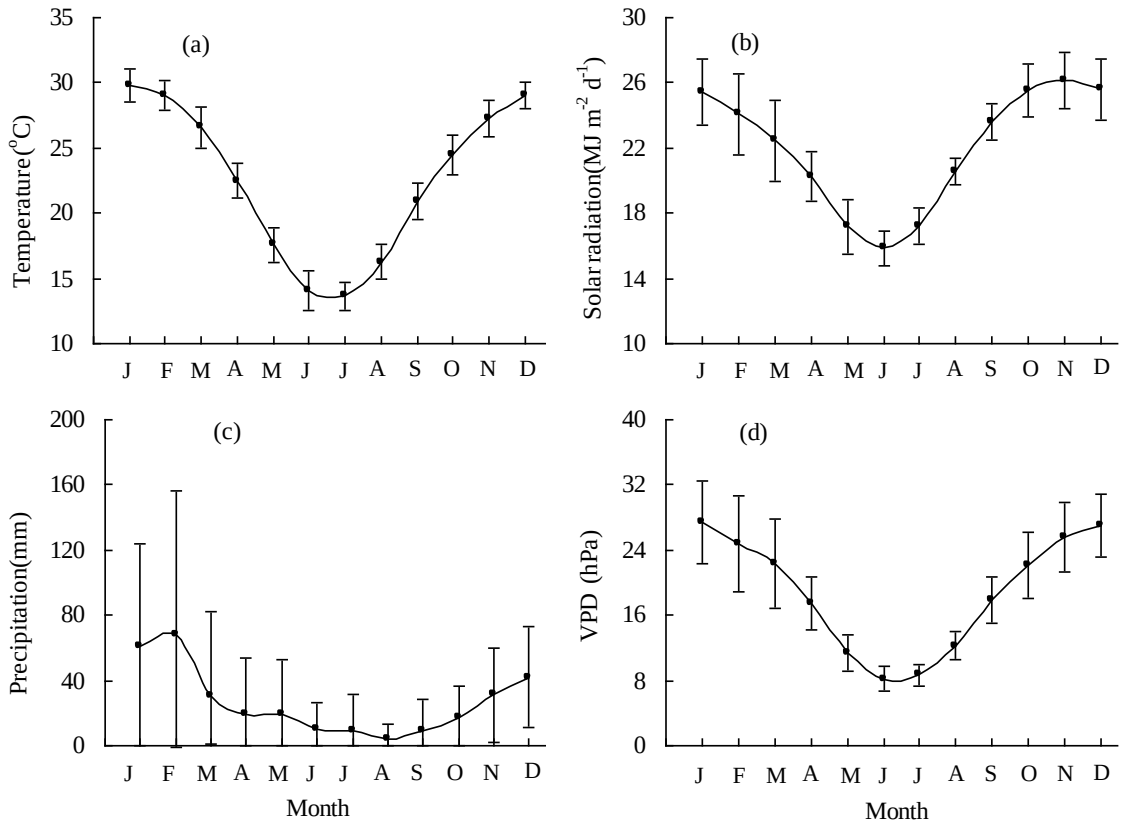

728

729 **Figure 7.** Mean monthly air temperature (a), mean monthly solar radiation (b), monthly precipitation

730 (c) and mean monthly vapour pressure deficit (VPD) (d).

731

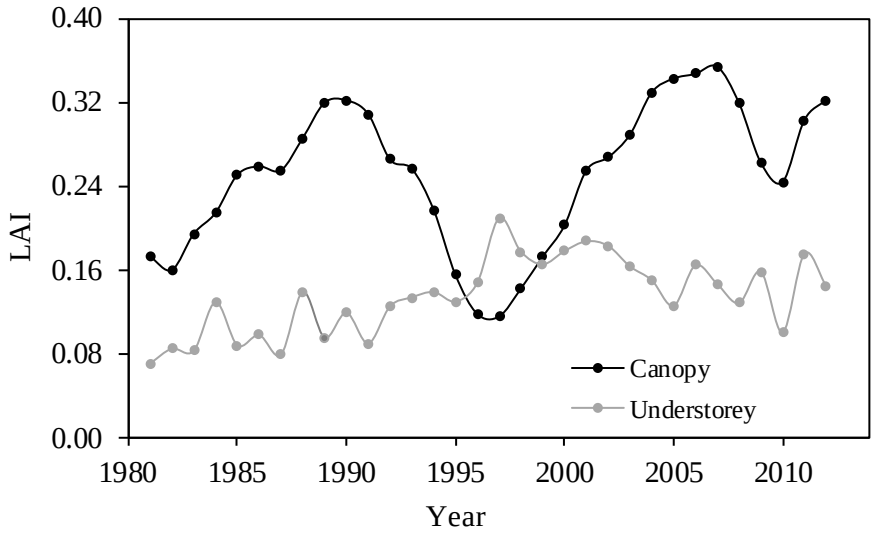

732

733 **Figure 8.** Simulated annual mean LAI of the canopy and understory from 1981 to 2012.

734

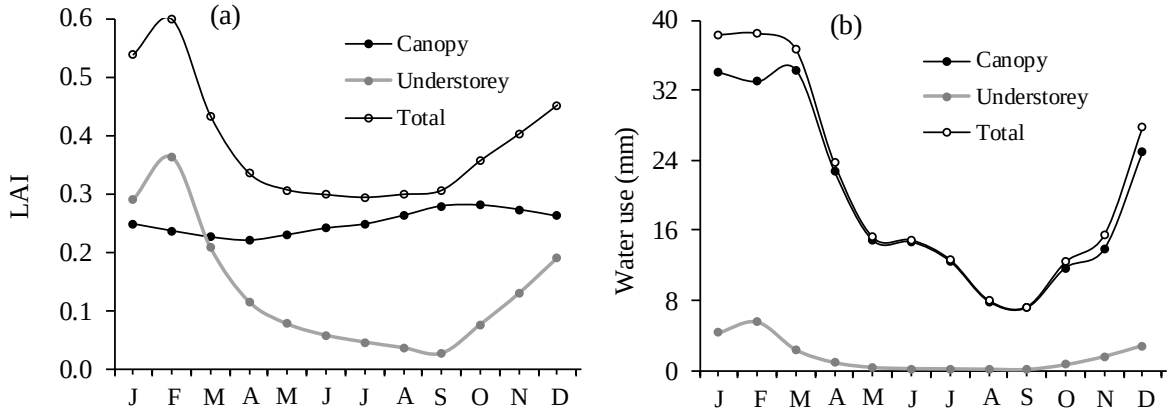

735

736 **Figure 9.** Simulated monthly mean LAI of the canopy, understory and their total (a); simulated

737 monthly water use of the Mulga, understory and their total (b).

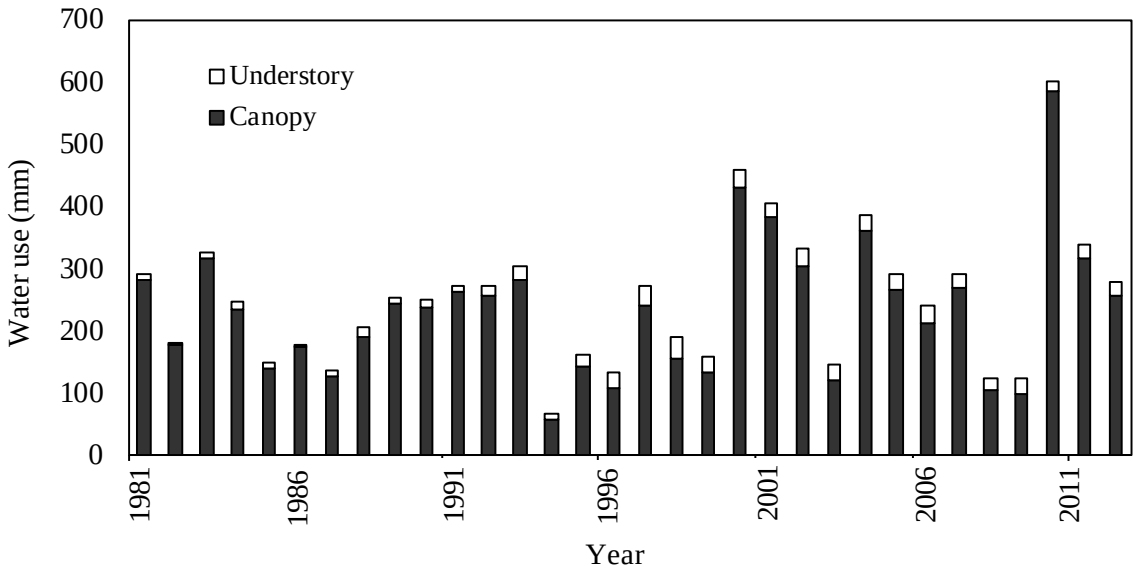

738

739 **Figure 10.** Simulated annual water use by the Mulga and understory from 1981 to 2012.

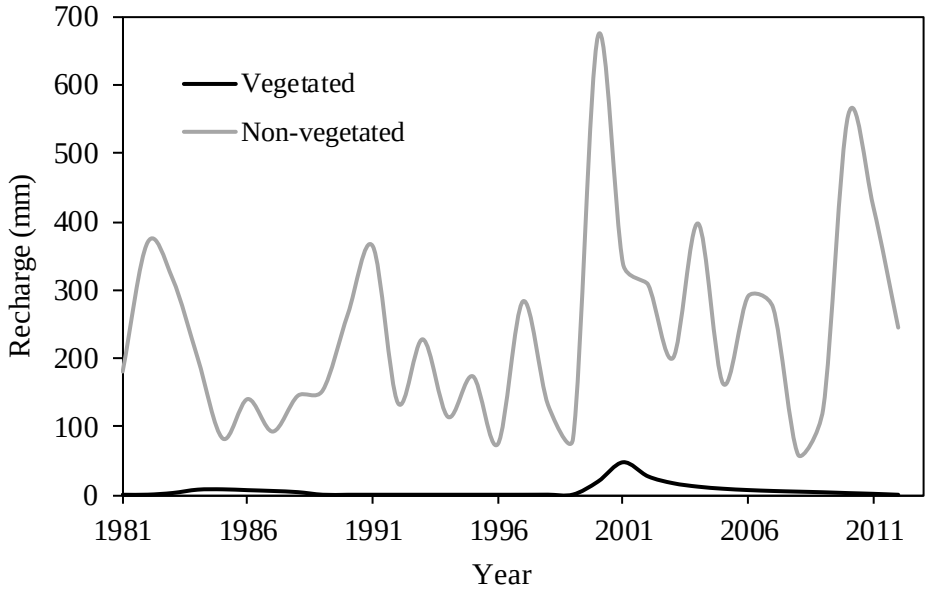

740

741 **Figure 11.** Simulated annual recharge with vegetation (vegetated) and without vegetation (non-
742 vegetated) during 1981–2012.

743

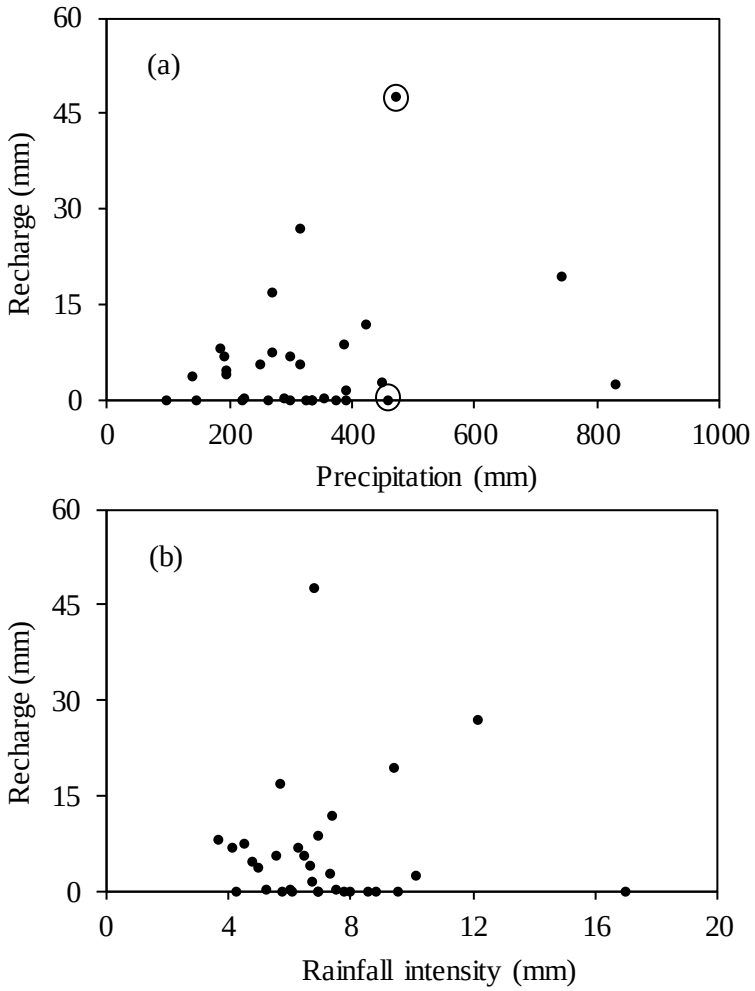

744

745 **Figure 12.** Relationships between annual recharge and annual precipitation (a) or rainfall intensity (b)
746 during 1981−2012. Rainfall intensity is calculated by computing the moving average of the daily
747 rainfall series applying a 7-day window, and then aggregating the averaged rainfall values that were
748 above a threshold of 5 mm d^{-1} (e.g., *Barron et al., 2012*).

749

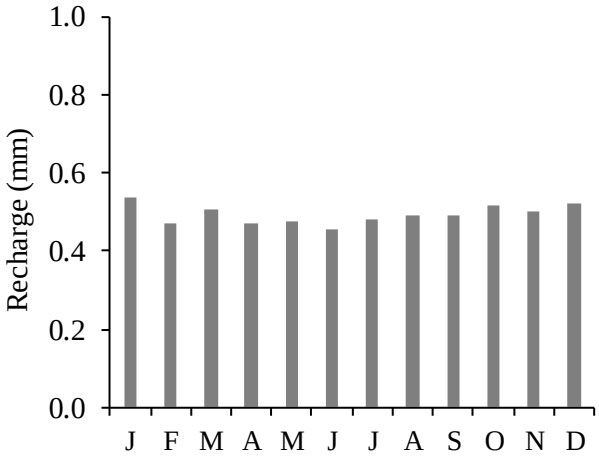

750

751 **Figure 13.** Simulated monthly recharge with vegetation during 1981−2012.

752

753 **Table 1**. Soil layers and parameters estimated for the soil model simulations

Soil layer	Soil depth (m)	Texture	Ks (m d^{-1})	Θ_s (cm^3 cm^{-3})	Θ_d (cm^3 cm^{-3})	λc (m)	C
1	0−4	sandy loam	1.0	0.33	0.06	0.04	1.02

754 Ks, saturated hydraulic conductivity

755 Θ_s, saturated soil water content

756 Θ_d, air-dry volumetric water content

757 λc, characteristic length

758 C, shape parameter related to soil texture and structure

759

760 **Table 2.** Derived parameter values for the canopy and understory

Parameter	Unit	Mulga	Understory
1 minus albedo of the canopy	—	0.75	0.75
1 minus albedo of the soil	—	0.80	0.80
Rainfall interception coefficient	—	0.0001	0.0001
Light extinction coefficient	—	-0.65	-0.50
Maximum carbon simulation rate	kg C $^{-2}$ d^{-1}	0.028	0.01
Slope parameter for the conductance model	—	1.0	0.8
Maximum plant available soil water potential	m	-150	-150
IRM weighting of water	—	1	1
IRM weighting of nutrients	—	0.2	0.2
Ratio of stomatal to mesophyll conductance	—	0.03	0.8
Temperature when the growth is 1/2 of optimum	^{o}C	15	25
Temperature when the growth is optimum	^{o}C	17	30
Year day of germination	d	-1	310
Degree-daylight hours for growth	^{o}C hr	-1	47000
Saturation light intensity	mol m^{-2} d^{-1}	1800	1800
Maximum rooting depth	m	4	0.75
Specific leaf area	LAI kg C^{-1}	17.5	24
Leaf respiration coefficient	kg C kg C^{-1}	0.0004	0.0004
Stem respiration coefficient		0.0001	-1
Root respiration coefficient		0.0001	0.0001
Leaf mortality rate	fraction of C d^{-1}	0.0004	0.0002
Above-ground partitioning factor	—	0.15	0.3
Salt sensitivity factor	—	0.5	0.5
Aerodynamic resistance	s m^{-1}	20	20

761

762

763 **Table 3.** The coefficient of determination, root mean square error (RMSE) and model efficiency (ME)
764 of simulated LAI, soil water and ET.

Item	r^2	RMSE	ME
Total LAI (MODIS)	0.54	0.10	0.41
Understory LAI (Observed)	0.93	0.04	0.85
Canopy LAI (Observed)	0.65	0.05	0.77
Soil water	0.70	0.03 cm^{-3} cm^{-3}	0.65
ET	0.98	1.07 mm d^{-1}	0.93

765 **Table 4.** Pearson correlation coefficients between climate variables and vegetation, LAI or recharge.

Time scale	Climate variables		LAI		Recharge with vegetation
			Canopy	Understory	
Inter-annual	Mean temperature		0.11	-0.15	-0.33
	Solar radiation		0.17	0.17	-0.34
	Rainfall	Total amount	0.01	0.03	0.26
		Intensity	−	−	0.06
	VPD		0.08	-0.28	-0.22
Seasonal	Mean temperature		0.08	0.80**	−
	Solar radiation		0.52	0.50	−
	Precipitation (total amount)		-0.20	0.97**	−
	VPD		0.23	0.72**	−

766 VPD, vapour pressure deficit

767 ** Correlations are significant with $p < 0.01$